

# Block Ionomer Micelles in Solution. 1. Characterization of Ionic Cores by Small-Angle X-ray Scattering

Diep Nguyen,<sup>†</sup> Claudine E. Williams,<sup>‡</sup> and Adi Eisenberg<sup>\*†</sup>

Department of Chemistry, McGill University, Montreal, Quebec, Canada H3A 2K6, and  
Laboratoire pour l'Utilisation du Rayonnement Électromagnétique (LURE),  
CNRS-CEA-MEN, Université Paris-Sud, 91405 Orsay Cedex, France

Received January 7, 1994; Revised Manuscript Received May 20, 1994\*

**ABSTRACT:** Diblock ionomers of polystyrene-*b*-poly(cesium acrylate) and polystyrene-*b*-poly(cesium methacrylate) in toluene, a solvent selective for the polystyrene blocks, were investigated by small-angle X-ray scattering (SAXS). The insoluble poly(cesium acrylate) and poly(cesium methacrylate) blocks are found to be assembled in spherical microdomains, surrounded by a styrene corona, a morphology analogous to that of reverse micelles. In the range of polymer concentrations from 0.01 to 0.1 g/mL, the polymeric micelles show an increasing degree of organization in the solution, as evidenced by up to three peaks in the SAXS profiles. Since the electron density of the ionic core is much larger than those of either the corona or the solvent, the X-ray scattering comes from the core only. Furthermore, the sizes of the cores are much smaller than the distances between them; thus, the features corresponding to the form factor and the structure factor appear in different regions of the scattering profile, leading to an unambiguous interpretation. The core radius is found to vary as the  $^{3/5}$  power of the number of the ionic units,  $N_B$ , as predicted by Halperin's star model for polymeric micelles. The aggregation number varies as  $N_B^{4/5}$  while the surface area per chain scales as  $N_B^{2/5}$ . The polydispersity in the core radius of these micelles is of the order of 1.03, much smaller than the distribution in the length of the individual ionic blocks.

## Introduction

Block copolymers in solutions have received much attention, both experimentally<sup>1-10</sup> and theoretically.<sup>11-20</sup> This is due to their special characteristics, namely the incompatibility resulting from the difference in solubility properties between the individual segments. A consequence of this is microphase separation, which, in the case of highly asymmetric block copolymers in solvents selective for the major component, results in the formation of micelle-like aggregates consisting of a core of the insoluble (minor) component surrounded by a corona of soluble chains. In ionic block copolymers, i.e., block copolymers in which one of the blocks is ionic, the tendency toward phase separation is even stronger. Diblock ionomers, in which the volume fraction of the ionic blocks is low,<sup>3,5</sup> have been shown to form stable reverse micelles in solvents selectively good for the nonionic components. It was also shown that the single chain fraction in solution is low<sup>3</sup> and that it decreases as the ionic block length increases.<sup>1</sup> Other studies were devoted to the diffusion of water into the core of the ionomer micelles<sup>2</sup> as well as to critical micellization phenomena.<sup>21</sup>

The ionomer micelles are, in many ways, similar to latex particles with long grafted polymer chains (hairy ball<sup>17</sup>) and also, to a lesser extent, to star polymers.<sup>19</sup> One advantageous feature of the block ionomer micelles lies in the fact that the size of the core is controlled by molecular parameters such as the length of the ionic blocks and can be varied over a wide range down to nanometer size.

Many models and theories have been published which deal with the morphology of block copolymer micelles.<sup>11-20</sup> Of particular relevance to the present work is Halperin's starlike model<sup>16</sup> for polymeric micelles which consist of a small inner core of insoluble B blocks and a swollen corona of soluble A blocks. The chain conformation in the corona is described in a way similar to that of the Daoud-Cotton

star model.<sup>19</sup> In the case when  $N_A \gg N_B$ , where  $N_A$  and  $N_B$  are the numbers of units per block, the structure of a single micelle is determined by a balance between the interfacial energy between the core and the corona and the free energy penalty due to chain extension in the corona. The energy contribution of the core is shown to be negligible and the size of the micelle is essentially set by the corona. The model predicts that the radius of the core,  $R$ , scales as  $N_B^{3/5}$  and that aggregation number  $N$  scales as  $N_B^{4/5}$ .

To test these predictions experimentally, one has to employ methods which allow one to probe the core directly. For the block ionomer micelles, the most suitable method is small-angle X-ray scattering (SAXS). Because of the high contrast between the ionic core on the one hand and the corona and solvent on the other, the scattering is due essentially to the core. Furthermore, the contrast can be varied by changing the cations (in the core) or by changing the solvents. Finally, the core sizes can be varied by changing the molecular weight of the ionic block. In the case where the ionic block length is short, the size of the core is much smaller than the size of the whole micelle; therefore, the characteristic lengths related to the size and the order are very different, and the corresponding scattering features appear in different regions of the pattern.

The present paper is devoted to a study by SAXS of block ionomer micelles of highly asymmetric AB diblock ionomers of polystyrene-*b*-poly(cesium acrylate) and polystyrene-*b*-poly(cesium methacrylate) in toluene. Specifically, the size and polydispersity of the ionic cores will be explored as a function of ionic block length, and an attempt will be made to fit the results to the star model. A future paper<sup>22</sup> will address the structure of micelles in solutions, the variation in the core sizes as a function of polystyrene block lengths, and the effect of different solvents. The topics of the interphase thickness of the microdomains and the results from solutions of polystyrene-*b*-poly(4-vinylpyridinium methyl iodide) will also be addressed in that paper.

\* To whom correspondence should be addressed.

<sup>†</sup> Department of Chemistry, McGill University.

<sup>‡</sup> LURE, CNRS-CEA-MEN, Université Paris-Sud.

\* Abstract published in *Advance ACS Abstracts*, July 1, 1994.

**Table 1. Parameters for Diblock Ionomers at 5% Concentration**

no. of PS units	no. of PACs units	$M_w/M_n^a$	$R_{core}^b$ (Å)	$N^c$ (agg no.)	$S/N^c$ (Å <sup>2</sup> /chain)	RPI <sup>d</sup>
190	3.8		18	38	110	
190	11	1.10	37	120	140	
190	24	1.13	44	88	280	1.04
600	45	1.20	54	87	420	1.02
630	4.2		18	34	120	
630	17	1.12	39	86	220	
630	31	1.12	56	140	280	1.03
1600	82	1.13	89	210	470	1.04
2300	31	1.12	52	110	300	1.04

no. of PS units	no. of PMACs units	$M_w/M_n^a$	$R_{core}^b$ (Å)	$N^c$ (agg no.)	$S/N^c$ (Å <sup>2</sup> /chain)	RPI <sup>d</sup>
170	9	2.7	25	35	220	
170	25	1.8	45	74	350	

<sup>a</sup> From SEC measurements of the ester form. Samples with very short ester blocks were not measured. <sup>b</sup> Calculated from eq 1 (see text). <sup>c</sup> Calculated from  $R_{core}$ . <sup>d</sup> Obtained from the fit of eq 1 modified by Gaussian polydispersity.

## Experimental Section

The block copolymers in this work were synthesized in connection with two other projects,<sup>1,6</sup> and their preparation has been described in detail elsewhere;<sup>1</sup> hence, only a summary is given here. The block copolymers of polystyrene-*b*-poly(*tert*-butyl acrylate or *tert*-butyl methacrylate) were synthesized by anionic polymerization. The initiator used was the reaction product of *sec*-butyllithium with a few units of  $\alpha$ -methylstyrene. These block copolymers were hydrolyzed to polystyrene-*b*-poly(acrylic acid) (PS-*b*-PAA) or polystyrene-*b*-poly(methacrylic acid) (PS-*b*-PMAA) by using *p*-toluenesulfonic acid as the catalyst in toluene solution. The polymers were recovered by precipitation into cold methanol and were then dried in a vacuum oven at 50 °C for 48 h. The composition of the copolymers was determined either by FTIR using copolymers in the ester form or by titration of the acid. The polydispersity indexes of all the polystyrenes and their copolymers, as determined by SEC, varied between 1.10 and 1.13. Different series of samples with different polystyrene (PS) block lengths and with different poly(acrylic acid) (PAA) or poly(methacrylic acid) (PMAA) lengths were prepared; the details are given in Table 1. The ratio of the ionic block lengths to the PS lengths varied from 0.5 to 13%.

The dried copolymers of PS-*b*-PAA and PS-*b*-PMAA were dissolved in benzene/methanol (90/10 v/v) at a concentration of about 2% (w/w). The acid was neutralized by addition of a stoichiometric amount of CsOH in methanol. The solutions were stirred for 1–2 h, and the block ionomers were recovered by freeze-drying. They were subsequently dried at 100 °C for 48 h under vacuum. The abbreviations used to indicate the copolymer composition are as follows: PS(600)-*b*-PACs(45) indicates a polystyrene chain of 600 units joined to a poly(acrylic acid) chain of 45 units neutralized with Cs.

Micellar solutions were obtained by dissolving the dried powder in the desired solvent. The polymer concentrations ranged from 1 to 10% by weight. For the SAXS experiment, the solution was enclosed in a 1.5 mm thick cell with 25  $\mu$ m thick Kapton windows.

The experiments were conducted at station D22, LURE-DCI, Orsay, using a synchrotron as the radiation source. A detailed description of the spectrometer is given elsewhere.<sup>23</sup> The angular range was chosen so as to provide data from  $q = 0.005 \text{ Å}^{-1}$  to  $q = 0.15 \text{ Å}^{-1}$  ( $q$  is the scattering vector, equal to  $4\pi \sin \theta / \lambda$ ,  $\theta$  is half the scattering angle, and  $\lambda$  is the X-ray wavelength). The resulting scattering intensities,  $I$ , were corrected for incident beam decay, sample thickness, and transmission. The background scattering from the solvent was also subtracted. The optics of the experimental setup were such that no desmearing of the curves was necessary.

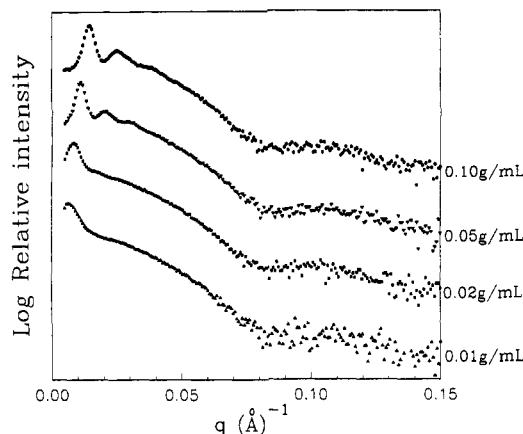


**Figure 1.** SAXS profiles of PS(600)-*b*-PACs(45) diblock ionomer in toluene in the concentration range from 0.01 to 0.10 g/mL.

## Results and Discussion

This part of the paper is divided into five sections. In the first section, the contrast for small-angle X-ray scattering is covered briefly. Then the description of the SAXS profiles is presented. In the third section, the shape factor features are discussed. The procedure to fit the SAXS profiles to obtain polydispersity indexes for core sizes is explained in section four. Finally, the Halperin model and its applicability to the present system are discussed.

**1. Contrast for X-ray Scattering.** X-ray scattering is due to the contrast provided by the difference in electron densities in the two media. In the system investigated here, the electron density of the PACs core is  $0.543 \text{ e/Å}^3$ , that of the PS corona is  $0.343 \text{ e/Å}^3$ , and that of the toluene solvent is  $0.282 \text{ e/Å}^3$ . In the calculation of these electron densities, the following polymer densities were used:  $1.06 \text{ g/cm}^3$  for polystyrene,<sup>24</sup>  $0.820 \text{ g/cm}^3$  for toluene,<sup>24</sup> and  $2.0 \text{ g/cm}^3$  for poly(cesium acrylate).<sup>22</sup> The presence of the heavy cation, Cs<sup>+</sup>, in the core creates a big difference in electron density between the core on the one hand and the corona and the solvent on the other. Furthermore, since the PS corona has an electron density similar to that of toluene, the solution can be approximated as a two electron density system, in which scattering is due essentially to the core.

**2. The SAXS Profiles.** SAXS profiles for the PS-(600)-*b*-PACs(45) sample in the concentration range 1–10% are presented in Figure 1. The behavior is typical of all the samples studied. Two distinct regions can be observed; for example, for this particular diblock, the first region extends from  $q \sim 0.005 \text{ Å}^{-1}$  to  $q \sim 0.05 \text{ Å}^{-1}$  and the second from  $q \sim 0.05 \text{ Å}^{-1}$  to  $q \sim 0.15 \text{ Å}^{-1}$ . In the first region, for the 5 and 10% solutions, three peaks can be seen which decrease in intensity and increase in peak width progressively with increasing  $q$ . The ratio of the  $q$  values at the maxima of these three peaks is approximately 1:1.8:2.7. For the 2% solution, the intensities of the second and third peaks decrease considerably, and for the 1% solution, only one peak is seen. The peaks in the first region move to lower  $q$  values as the concentration decreases, which indicates that they are due to order in the solution; the scattering in the first region can thus be regarded as reflective of the structure pattern of the micelle solutions. The first peak is related to an average distance between scattering centers, and it is verified that its position  $q_{max}$  varies as  $c^{1/3}$ , as expected from spherical objects on a 3-D lattice. Since the low  $q$  region provides no information on single micelle characterization, it will not be discussed any further in this paper.

In the second region a pronounced curvature is followed by a shallow minimum around  $q$  values of  $0.08 \text{ \AA}^{-1}$  and by a very broad peak; this behavior is observed for all solutions down to a concentration of 2%. For the 1% solution, the signal is noisy, and the minimum and the broad peak are not well defined. The position of the shallow minimum and that of the maximum of the broad peak do not change with concentration of the solutions. Since the shape factor peak is determined only by the size of the sphere, its position should not change with the concentration, as is observed for the features in the second region; thus, it can be concluded that this region is dominated by the scattering from the shape factor for spheres. It should be noted that the  $q$  range for each region depends on the relative block lengths of the two blocks.

**3. The Shape Factor Peaks.** In general, for an assembly of scattering particles, the scattered intensity,  $I(q)$ , is the product of the particle shape factor,  $P(q)$ , and the structure factor,  $S(q)$ , which characterizes the spatial correlation of the scatterers. Since it is a product of two functions, it is often difficult to separate one from the other experimentally. In the present system, since the sizes of the spheres are so much smaller than the characteristic distances between them and since the contrast between the two media is substantial, the attribution is unambiguous. As was mentioned before, the scattering in the second region is attributed to the shape factor for spheres. It is worth recalling here that the equation for the scattering intensity due to monodisperse spheres is

$$P(q) \cong \left[ \frac{3 \frac{\sin(qR) - qR \cos(qR)}{(qR)^3} \right]^2 \quad (1)$$

Equation 1 has minima (zeros) at  $qR = 4.5, 7.7$ , etc. From the position of these minima one can determine the radius of the spheres.

**4. Polydispersity Fit.** While the shape factors give sizes directly, polydispersity or deviation from sphericity smears out the features in a similar way.<sup>25</sup> In the present system, since the volume fraction of the ionic block is low (below 12%) and since the micelles of diblock ionomers of similar structure have been shown to be spherical,<sup>3,6</sup> the absence of a deep minimum and the fading out of the form factor features are assumed to result only from the polydispersity of sphere sizes. Hence the high  $q$  region of the SAXS profiles was fitted by eq 1 modified for polydispersity and assuming a Gaussian distribution.<sup>26</sup>

The fit of the SAXS profile in the shape factor region was carried out as follows: first the radius was obtained from the position of the minimum or maximum; then, different shape factor plots for this radius with different radii polydispersity indexes, RPI, were generated. The plot which gave the lowest  $\chi^2$  value for the fit of both the shallow minimum and the broad peak of the experimental SAXS profile was chosen as the best fit. An example of the fit is shown in Figure 2. In this figure, the shape factor plots for monodisperse spheres (RPI of 1 or  $\sigma = 0 \text{ \AA}$ , where  $\sigma$  is the standard deviation) and the shape factor for spheres with polydispersities of RPI of 1.02 ( $\sigma = 8.5 \text{ \AA}$ ) and 1.05 ( $\sigma = 12.0 \text{ \AA}$ ) are shown. Clearly, the best fit to the experimental profile is the plot with the RPI of 1.02. It should be mentioned that for a RPI of 1.1 the shape factor peaks are completely smeared out.

It should be noted that not all the SAXS profiles can be fitted so as to obtain the polydispersity unambiguously. Only those with the best signal to noise ratio can give reliable results; for those profiles in which the signal for the broad shape peak is very noisy as is seen, for example,

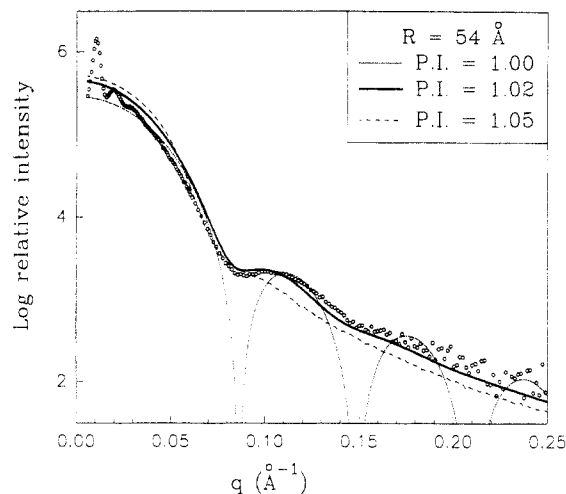


**Figure 2.** SAXS profile for the 0.05 g/mL solution of PS(600)-b-PACs(45) in toluene and fits for a radius of 54 Å with radius polydispersity indexes of 1.00 (eq 1), 1.02, and 1.05.

for solutions below a concentration of 5%, a fit is more difficult to obtain. In these cases, the strong curvature at low  $q$  is used to fit eq 1 to obtain the core radius. The values of the core radii,  $R$ , and of the polydispersities, when available, are listed in Table 1 for solutions at a 5 wt % concentration. It is to be noted that the polydispersity in core sizes does not change with concentration. For example, for PS(600)-PACs(45) the RPI at 10 and 5% concentration is 1.03 for both cases. This is reasonable, since as the solutions become dilute, the sizes of the core should not be affected and only the distances between the micelles should increase, as was indeed observed. It should be noted that RPI values of the core radii are lower than the polydispersities of the different diblocks, which varied from 1.12 to 1.20. The method of sample preparation may affect the polydispersity of the micelles. An investigation of this effect is underway.<sup>27</sup> It is worth mentioning here that in a study of the polydispersity of domain sizes in relation to that of the individual block copolymers in the solid state, Hashimoto *et al.* had reported the same finding.<sup>28</sup>

**5. Application of the Halperin Model.** From the values of  $R$  and the density of the ionic block,<sup>22</sup> one can calculate the aggregation number,  $N$ , and the surface area per chain,  $S/N$ , for the micelles. These values are reported in Table 1 for various copolymer compositions at a 5% concentration. Recall that no effect of concentration has been observed in the 1–10% range. It can be seen that the changes in radii for the different ionic block lengths are significant; in contrast to this, there is no dramatic change in the radii for the different PS block lengths.

One of the goals of this paper is to examine the data in terms of Halperin's model for starlike micelles<sup>16</sup> which predicts the scaling law for the core size and the aggregation number as  $R \propto aN_B^{3/5}$  and  $N \propto aN_B^{4/5}$ . From these relations it follows that  $S/N$ , the surface area per chain, scales as  $N_B^{2/5}$ .

The experimental values of  $R$  have been plotted as a function of  $N_B^{3/5}$  for PACs and PMACs cores (Figure 3). They fit a straight line, implying that the star model is, indeed, adequate to describe this system. Plots of  $N$  vs  $N_B^{4/5}$  and  $S/N$  vs  $N_B^{2/5}$  (not shown) are also linear but exhibit a somewhat higher scatter because a power of the radius is involved in the calculation of these data, i.e., a second power for  $S/N$  and a third power for  $N$ .

This model relies on some assumptions; first, the core must be much smaller than the corona, second, the

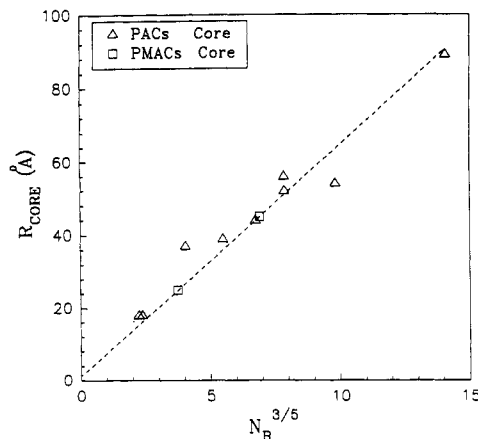


Figure 3. Plot of  $R_{\text{core}}$  (Å) vs  $N_B^{3/5}$  ( $N_B$  is the number of units in the ionic block).

interface between the core and the corona must be sharp, and last, the core should be meltlike. Do the ionomer micelles violate any of these assumptions? It is generally difficult to form stable polymeric micelles with small cores and to be able to vary the core sizes over a wide range. In this respect, block ionomers are ideal in that they form stable micelles in a selective solvent for the nonionic block even at very short ionic block lengths, down to a few units, and at very low polymer concentrations.<sup>1,3</sup> In a study of PS-*b*-PAA diblock ionomers of comparable volume fraction of the ionic content by light scattering, the cmc was found to be around  $10^{-8}$  M.<sup>27</sup> In this report, the lowest concentration studied was 1%, which is far above the cmc of the system;<sup>1,29</sup> the highest concentration was 10%, at which point the solutions were clear but very viscous. In addition to this, it was found in this study that the intensities at high angle varied as  $q^{-4}$ , which suggests that the interface between the core and the corona is sharp, as in the case for block ionomers in the solid state investigated before.<sup>29,30</sup> It should be noted here that the core was above its  $T_g$  when the acid diblocks were being neutralized, which was when the micelles were formed.

It should be mentioned that the proportionality constant between  $R$  and  $N_B^{3/5}$  found here is 6.5 Å. It appears that this length is closer to the statistical length of the polymer. The value found here is equal to 2–3 monomer units if the monomer size is taken to be 2.5 Å.

## Conclusions

Block ionomers are an excellent system for the investigation of the morphology of polymeric micelles in solution. Block ionomers, in a solvent selective for the nonionic blocks, form micelles even at very short ionic block lengths and at very low polymer concentrations; thus, they can provide a system of micelles with nanometer-scale cores which are very stable. SAXS is a most suitable method for the study of block ionomer micelles in solution; the advantages are the substantial difference in electron densities and the difference in magnitudes between the sizes of the cores and the distances between the scattering centers, which leads to a clear separation in the scattering pattern between the shape factor features and those due to structure factors. This allows for an unambiguous

interpretation of the data. It was found that the radii, the aggregation numbers, and the surface area per chain of these block ionomer micelles follow the scaling arguments of the Halperin star model for polymeric micelles. Finally, the polydispersity in core sizes for the micelles was found to be low, around 1.03–1.05, considerably smaller than the polydispersity of the polymer chains.

**Acknowledgment.** Valuable comments from Dr. A. Halperin are greatly appreciated. We thank Dr. A. Desjardins for the PS-*b*-PMAA diblocks and Dr. S. K. Varshney for the PS-*b*-PAA diblocks which had been prepared in connection with other projects. We thank Mr. F. Bossé for the BASIC computer program. D.N. is grateful to Le Fonds pour la Formation de Chercheurs et l'Aide à la Recherche (Quebec) for graduate scholarships.

## References and Notes

- (1) Zhong, X. F.; Varsheny, S. K.; Eisenberg, A. *Macromolecules* 1992, 25, 7160.
- (2) Gao, Z.; Desjardins, A.; Eisenberg, A. *Macromolecules* 1992, 25, 1300.
- (3) Desjardins, A.; van de Ven, T. G. M.; Eisenberg, A. *Macromolecules* 1992, 25, 2412.
- (4) Xu, R.; Winnik, M. A.; Riess, G.; Chu, B.; Croucher, M. D. *Macromolecules* 1992, 25, 644.
- (5) Cogan, A. K.; Gast, A. P.; Capel, M. *Macromolecules* 1991, 24, 6512.
- (6) Desjardins, A.; Eisenberg, A. *Macromolecules* 1991, 24, 5779.
- (7) Wang, J.; Wang, Z.; Peiffer, D. G.; Shuely, W. J.; Chu, B. *Macromolecules* 1991, 24, 790.
- (8) Pleštil, J.; Hlavatá, D.; Hrouz, J.; Tuzar, Z. *Polymer* 1990, 31, 2112.
- (9) Shibayama, M.; Hashimoto, T.; Kawai, H. *Macromolecules* 1983, 16, 16.
- (10) Selb, J.; Gallot, Y. In *Developments in Block Copolymers—2*; Goodman, I., Ed.; Elsevier Applied Science: London, 1985; Chapter 2.
- (11) Marko, J. F.; Rabin, Y. *Macromolecules* 1992, 25, 1503.
- (12) Birshtein, T. M.; Zhulina, E. B. *Polymer* 1989, 30, 170.
- (13) Marques, C.; Joanny, J. F.; Leibler, L. *Macromolecules* 1988, 21, 1051.
- (14) Fredrickson, G. H.; Helfand, E. *J. Chem. Phys.* 1987, 87, 697.
- (15) Bug, A. L. R.; Gates, M. E.; Sarfran, S. A.; Witten, T. A. *J. Chem. Phys.* 1987, 87, 1821.
- (16) Halperin, A. *Macromolecules* 1987, 20, 2943.
- (17) Witten, A.; Pincus, P. A. *Macromolecules* 1986, 19, 2509.
- (18) Noolandi, H.; Hong, K. M. *Macromolecules* 1983, 16, 1443.
- (19) Daoud, M.; Cotton, J. P. *J. Phys.* 1982, 43, 531.
- (20) Leibler, L.; Orland, H.; Wheeler, J. C. *J. Chem. Phys.* 1979, 7, 3550.
- (21) Khougaz, K.; Gao, Z.; Eisenberg, A. Manuscript in preparation.
- (22) Nguyen, D.; Williams, C. E.; Eisenberg, A. Manuscript in preparation.
- (23) Dubuisson, J. M.; Dauvergne, J. M.; Depautex, C.; Vachette, P.; Williams, C. E. *Nucl. Instrum. Methods Phys. Res.* 1986, A246, 636.
- (24) *Polymer Handbook*, 3rd ed.; Brandrup, J.; Immergut, E. H., Eds.; John Wiley and Sons: New York, 1989.
- (25) Glatter, O.; Kratky, O. In *Small Angle X-Ray Scattering*; Academic Press: New York, 1982.
- (26) Nguyen, D.; Bossé, F.; Williams, C. E.; Eisenberg, A. Manuscript in preparation.
- (27) Khougaz, K.; Eisenberg, A. Manuscript in preparation.
- (28) Hashimoto, T.; Tanaka, H.; Hasegawa, H. *Macromolecules* 1985, 18, 1864.
- (29) Gouin, J. P.; Williams, C. E.; Eisenberg, A. *Macromolecules* 1989, 22, 4573.
- (30) Gouin, J. P.; Bossé, F.; Nguyen, D.; Williams, C. E.; Eisenberg, A. *Macromolecules* 1993, 26, 7250.